

Fermilab Library



0 1160 0052489 6

SDC-90-00075

<p style="text-align: center;">SDC SOLENOIDAL DETECTOR NOTES</p>
--

MUON RATES FOR TRIGGERS

D. Green

August 1990

SDC NOTE # 90-00075

MUON RATES FOR TRIGGERS

**Dan Green
Fermi National Accelerator Laboratory*
P.O. Box 500
Batavia, Illinois 60510**

August 1990

The FNAL supported product SSCSIM has been used in order to evaluate muon trigger rates for SDC. The decays $\pi \rightarrow \mu\nu$ and $K \rightarrow \mu\nu$ were assumed to occur in a cylindrical void of radius 2.3m and half length 4.5m. This void was surrounded by shells of $10 \lambda_0$ thickness (calorimeter) and $4 \lambda_0$ (muon steel) in the barrel region, and $14 \lambda_0$, $8 \lambda_0$ in the end plug region.

The decays were performed with the full kinematics except that the μ direction was taken to be the parent direction. Energy loss was taken into account, but not multiple scattering. For the purposes of evaluating trigger rates these approximations are not debilitating. Punchthrough probabilities, $P(\lambda, P)$, were evaluated using a parametrization of the WA1 data,^[1] $P(\lambda, P) = \text{EXP}[(\lambda - \lambda')/\lambda_{\text{EFF}}]$. The momentum after punchthrough was evaluated using a fragmentation function, $D(Z) \propto (1-Z)^4/Z^2$, $k = ZP$, which is a good representation of all data.^[2] The punchthrough muon has the parent direction. The approximation is sufficient for the purposes of this note.

First the minbias, all charged, cross section was examined. An inelastic cross section of $\sigma_I = 100$ mb was assumed. A rapidity plateau density, $1/\sigma(d\sigma/dy) \sim 6$ was observed. The distribution in k_T at $y = 0$ is shown in Fig. 1.

Also shown in Fig. 1 is an estimate of the decay rate (dash-dot) found by multiplying by the factor $(Rm_\pi/p_T c\tau_\pi)$ and an estimate for the punchthrough rates given by multiplying the pion spectrum by $P(\lambda, P)$ for $\lambda = 10 \lambda_0$ (dotted) and $\lambda = 14 \lambda_0$ (dashed). These hand estimates are a reasonable approximation to the final results, as will be shown. Note that punchthrough dominates over decay for $k_T > 10$ GeV at $10 \lambda_0$ and for $k_T > 25$ GeV at $14 \lambda_0$.

The SSCSIM results for decays are shown in Fig. 2. The scale of nb/GeV converts to a trigger rate of Hz/GeV , per unit of rapidity on the plateau, at the SSC design luminosity. Clearly the estimates agree well, which serves as a crosscheck. In these figures k_T refers to transverse momentum at production; i.e., as measured in the tracker.

Results for $10 \lambda_0$ punchthrough are shown in Fig. 3. The curve (o) for $Z \equiv 1$ (tracker) dominates over decays (Fig. 2) for $k_T > 10$ GeV. The rates in the muon system (but referred back to the tracker) are also shown in Fig 3, (*). Clearly, at fixed k_T you buy a factor ~ 30 by remeasuring the momentum in the muon system. Even so, rates at $10 \lambda_0$ depth in the muon system are comparable to the decay rates. The situation is rapidly

improved with depth. At $14 \lambda_0$, Fig. 4, the overall punchthrough rates are reduced by a factor ~ 30 w.r.t. the $10 \lambda_0$ rates. Punchthrough as measured in the tracker dominates for $k_T > 20$ GeV. However, at $14 \lambda_0$ a remeasurement of k_T in the muon system insures that decays dominate at all k_T .

The angular dependence of the decay background (\bullet) is shown in Fig. 5. This rate rises by a factor of ten as y goes from 0 to 3. However, this rise is entirely due to low k_T leakage. As shown in Fig. 5, a cut on k_T at 2 GeV (\circ) yields a decay rate which is roughly constant in y . [In all of this discussion y is, in reality, the pseudorapidity $\eta = \ln(\tan(\theta/2))$]. The rise with y is due to the fact that a constant range cut, k_{min} , means a k_T cut, $(k_T)_{min} \sim k_{min} \theta$, which reduces as y increases.

The punchthrough rate, at fixed k_T , also rises about a factor of 10 as y goes from 0 to 3. In this case the rise is due to the rapid rise of $P(\lambda, P)$ with $P = P_T/\sin\theta$. However, since decays dominate, this fact is almost irrelevant to the trigger rate calculations.

The prompt muon spectrum from c , b , and t decays (combined) is shown in Fig. 7. A cross section for $c\bar{c}$ of 2.0 mb is assumed; a cross section for $b\bar{b}$ of 0.3 mb is assumed. Comparing to Fig. 2, one can see that real prompt muons from heavy flavors dominate all backgrounds for $k_T > 20$ GeV. The necessary conditions are a total absorber depth of $\geq 14 \lambda_0$ and a second muon measurement in exiting the absorber so as to reduce punchthroughs. No attempt has been made to simulate a "kink" cut in the central tracker. Therefore, one can anticipate a modest further reduction in the decay background.

The rapidity distributions for muons from heavy flavors are shown in Fig. 7. For both $c\bar{c}$ (\bullet) and $t\bar{t}$ (\circ) ($M_t = 150$ GeV) a "plateau" is observed of width, $\Delta y \sim \pm 1.5$. The plateau is slightly narrower for $t\bar{t}$ than $c\bar{c}$, a well known kinematic effect [$y_{MAX} \sim \ln(\sqrt{s}/M_Q)$]. The heavy flavor sources in SDC may clearly be considered to be spread roughly uniformly over the "barrel" region.

CONCLUSIONS

1. Without "exterior" measurement of momentum, punchthrough dominates over decays for $k_T \geq 10$ GeV ($10 \lambda_0$), $k_T \geq 20$ GeV ($14 \lambda_0$).
2. With "exterior" measurement, punchthrough is still \sim decay for $10 \lambda_0$, but decays dominate for $14 \lambda_0$.
3. Above k_T for the μ of about 20 GeV the $c\bar{c}$ rate exceeds the decay background. (~ 30 GeV for $b\bar{b}$). Real prompt rates from heavy flavors never exceed background rates without momentum remeasurement and sufficient absorber thickness ($l \geq 14 \lambda_0$).

REFERENCES

- ¹D. Green, "Muon Triggering at Small Angles," proc. of the Workshop on Triggering, Data Acquisition and Computing in Hadron-Hadron Colliders, Fermilab (1985).
 - ²D. Green and D. Hedin, "Muon Rates at the SSC," FNAL-PUB-90/18.
-

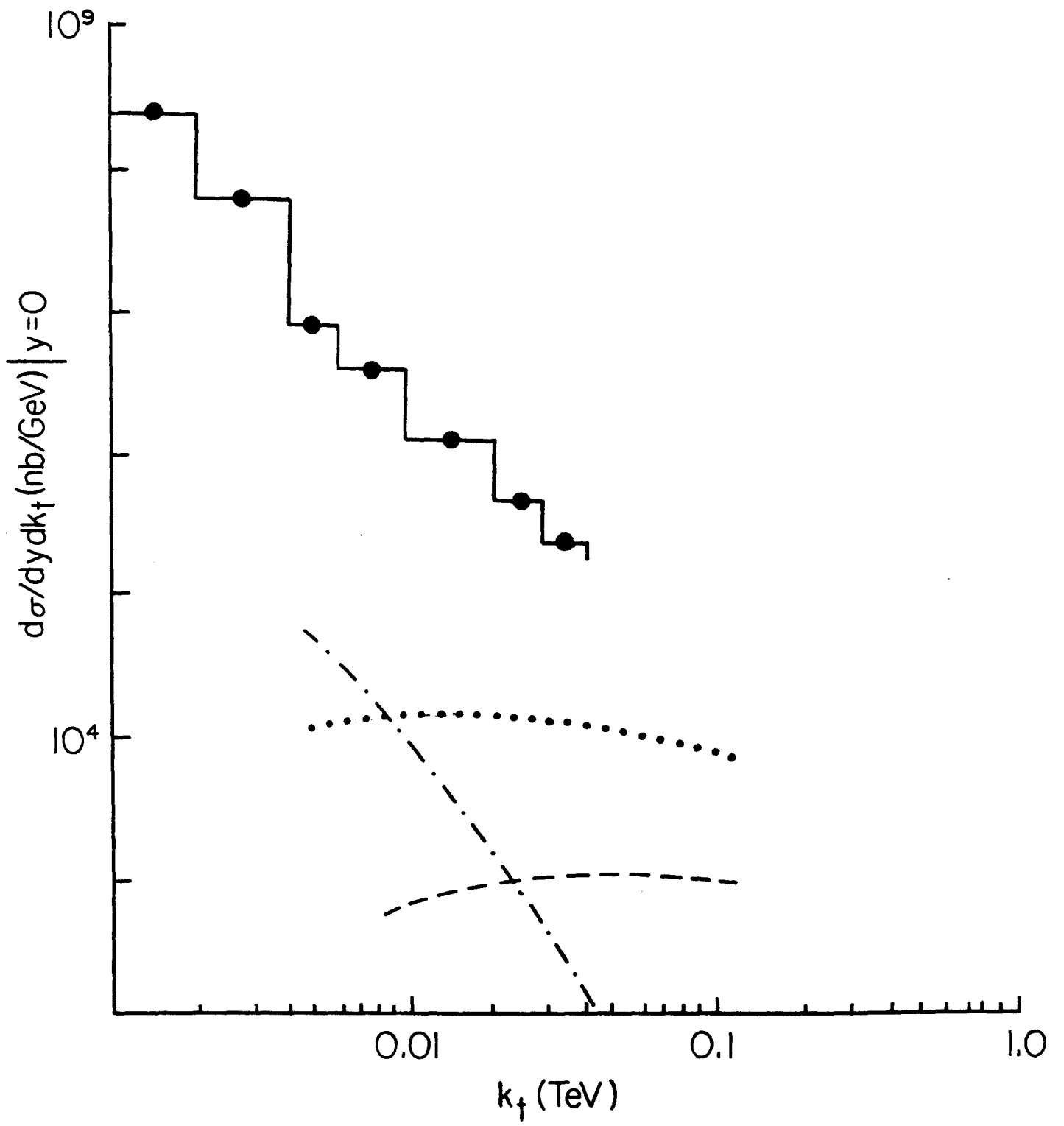


Figure 1

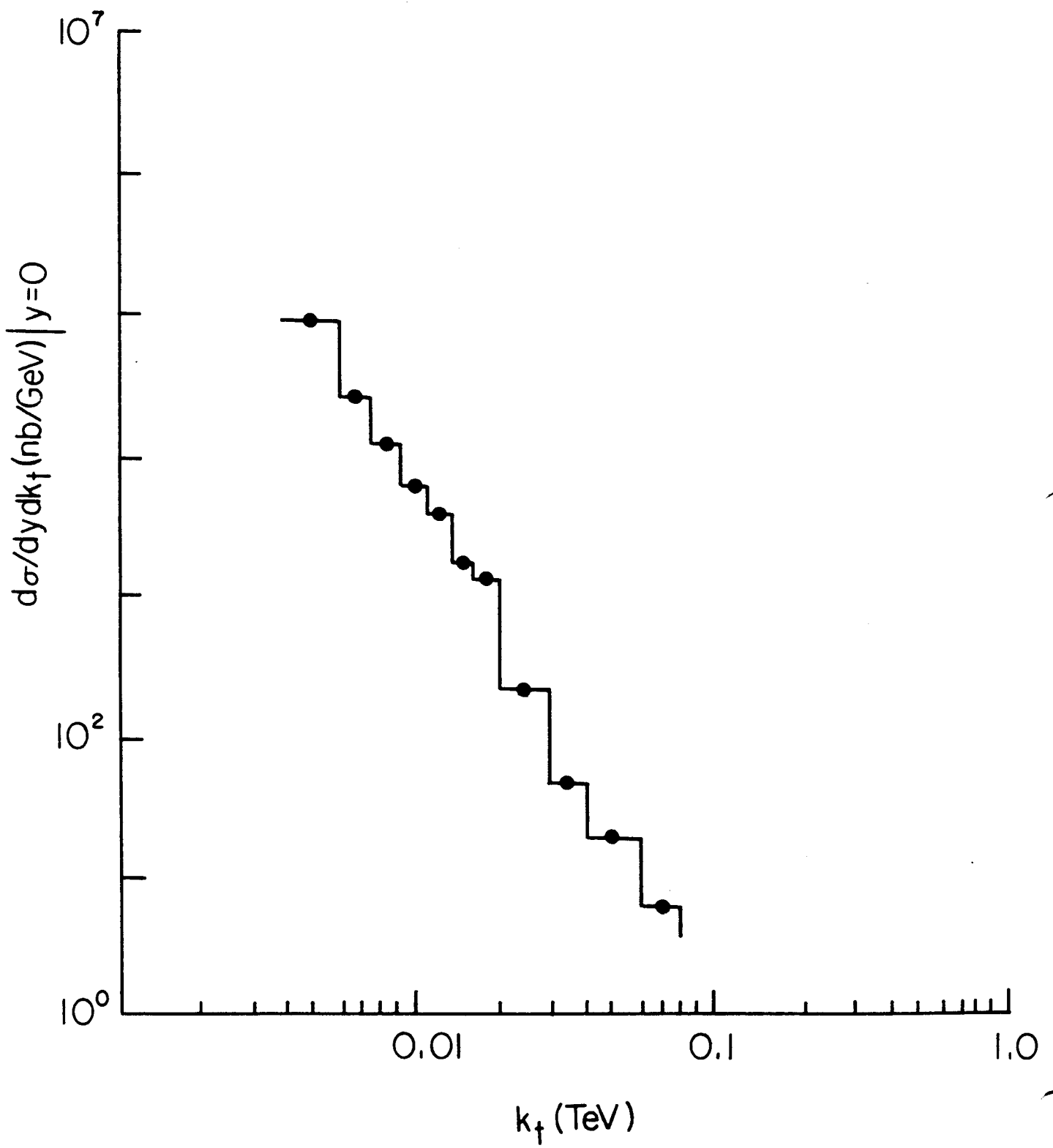


Figure 2

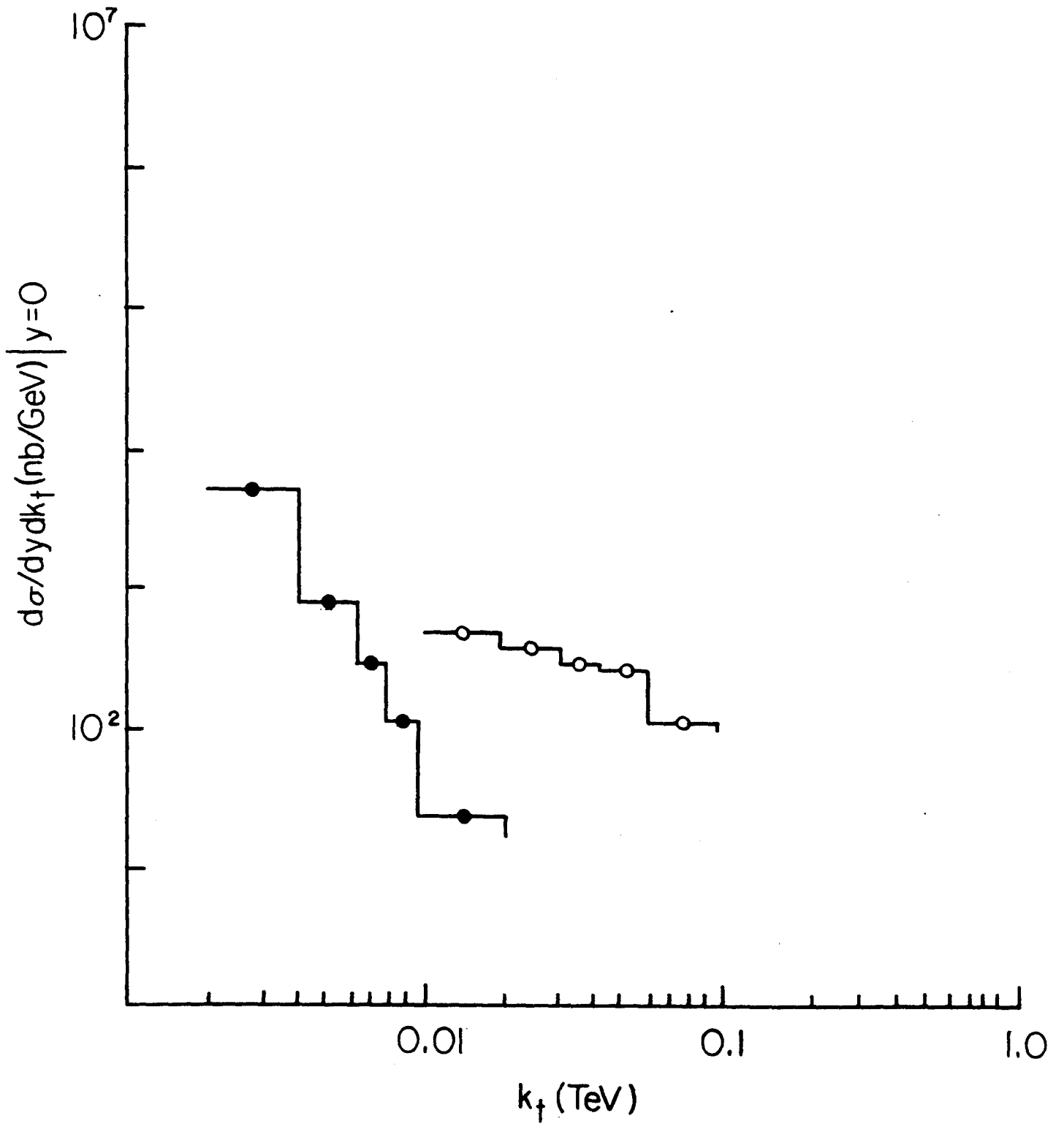


Figure 3

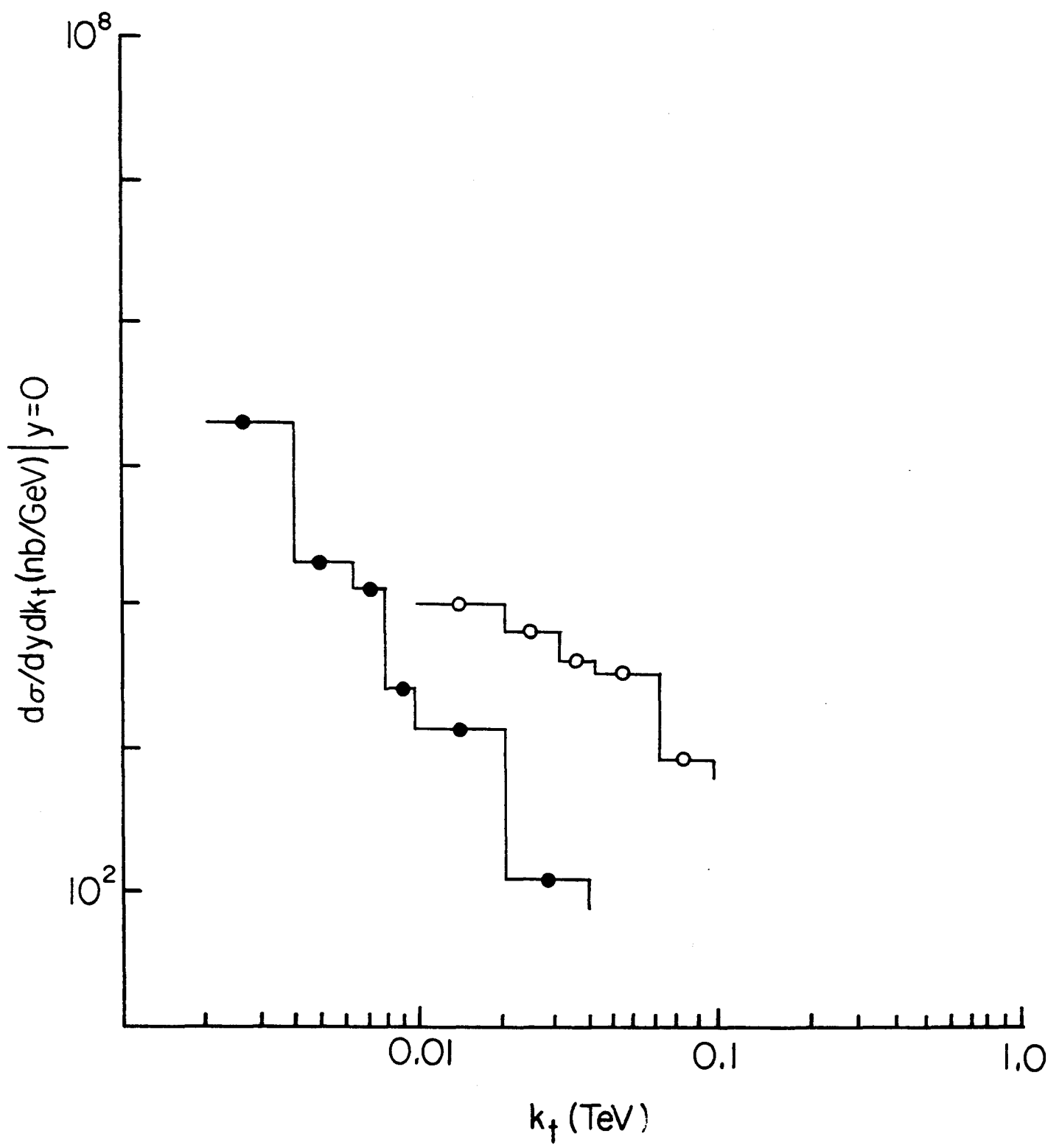


Figure 4

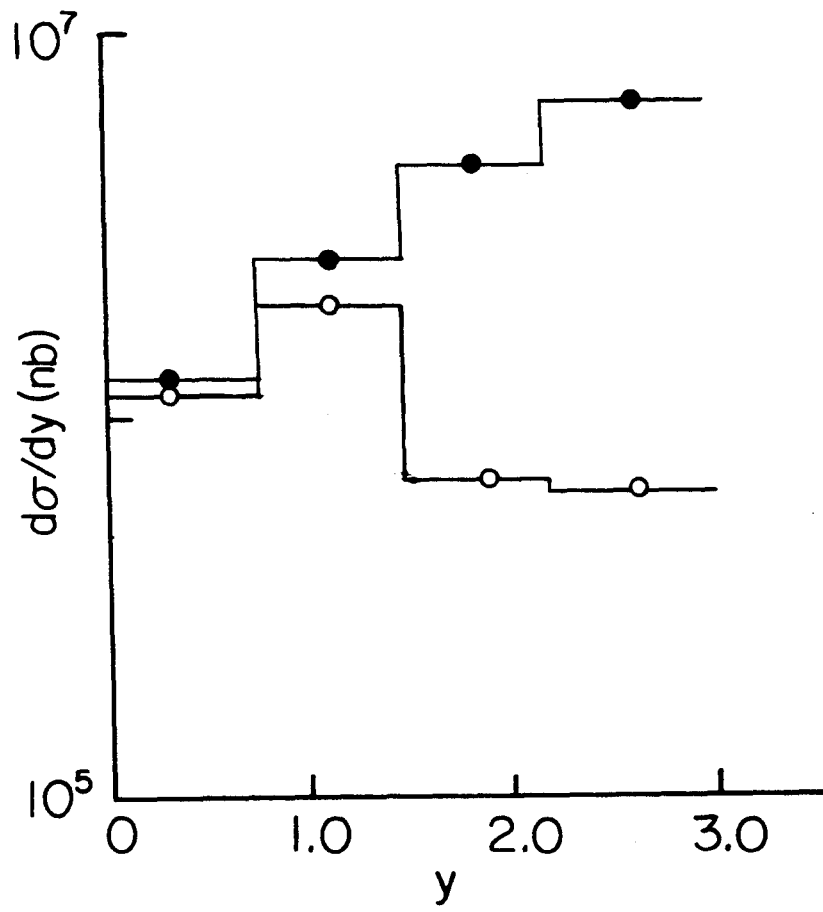


Figure 5

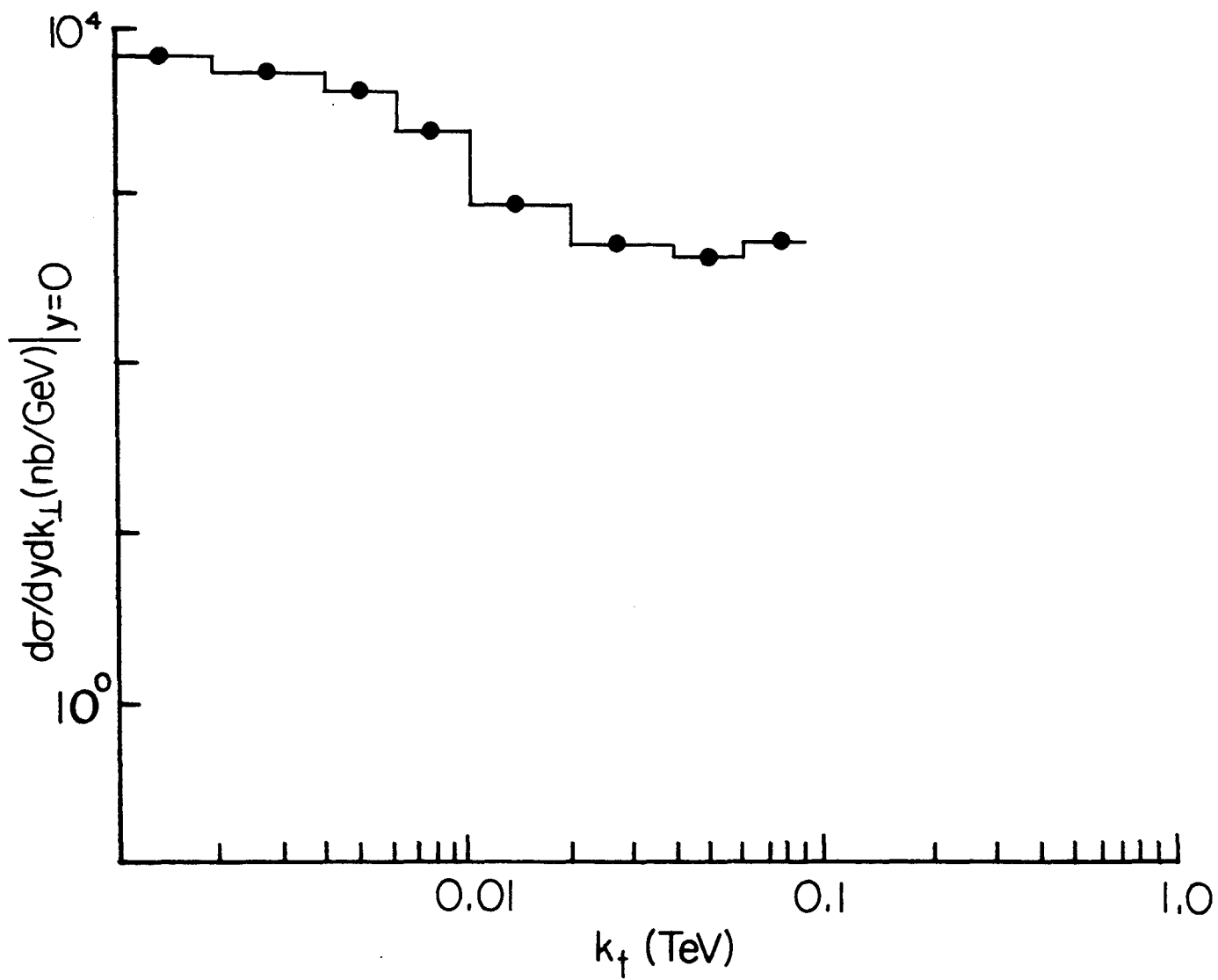


Figure 6

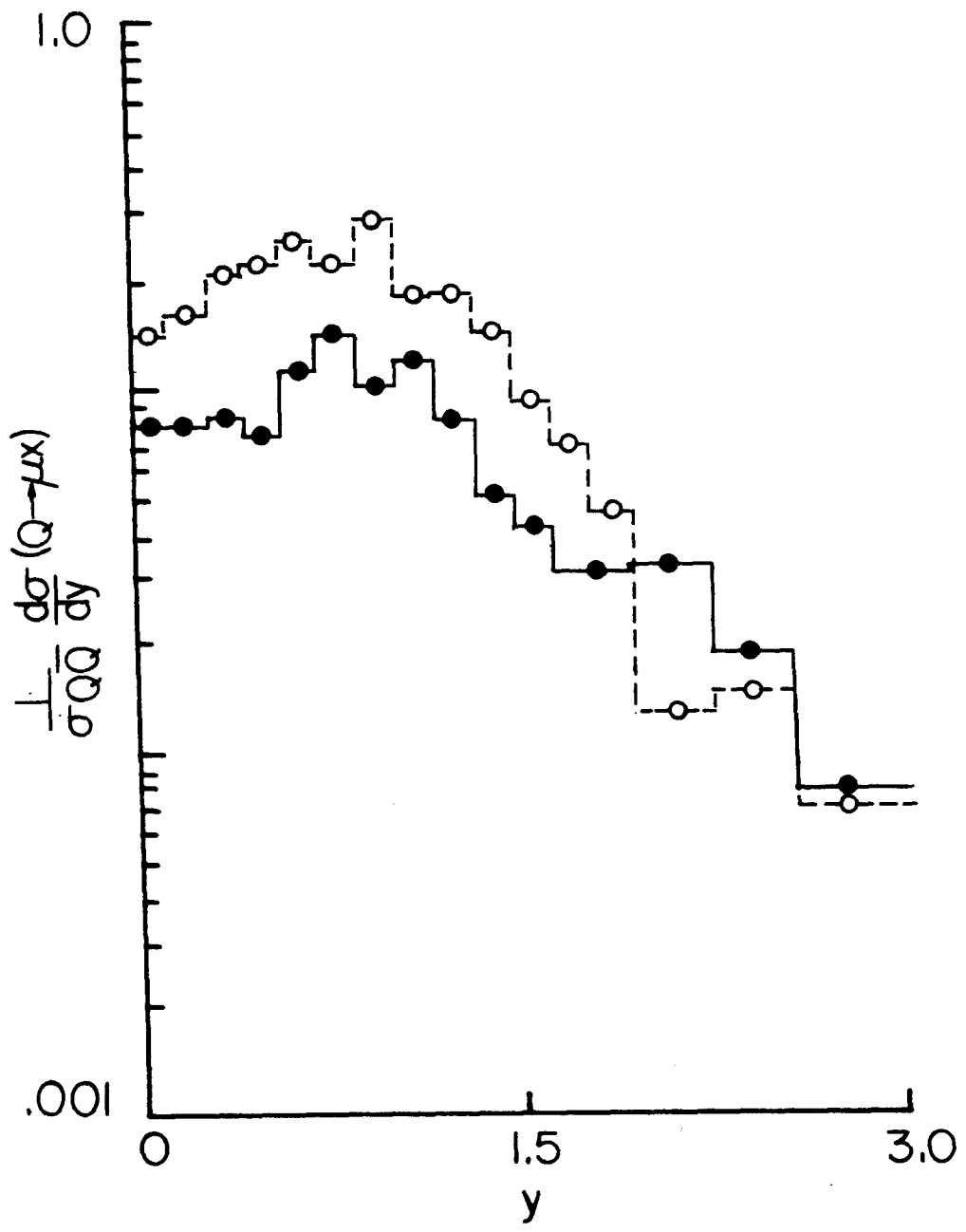


Figure 7